Available online at www.sciencedirect.com
ScienceDirect
Continental Shelf Research 27 (2007) 1893–1907
CONTINENTAL SHELF RESEARCH
www.elsevier.com/locate/csr

Hindered settling of mud flocs: Theory and validation

P.J.T. Dankers[a,ffi], J.C. Winterwerp[b,c]

[a]Hydraulic Engineering Section, Faculty of Civil Engineering and Applied Geo-Sciences, Delft University of Technology, P.O. Box 5048, 2600 GA, Delft, The Netherlands
[b]Section of Environmental Fluid Mechanics, Faculty of Civil Engineering and Applied Geo-Sciences, Delft University of Technology, Delft, The Netherlands
[c]WLkDelft Hydraulics, Delft, The Netherlands

Received 15 December 2005; received in revised form 14 March 2007; accepted 28 March 2007
Available online 14 April 2007

Abstract

This paper deals with settling of highly concentrated cohesive sediment suspensions. We evaluate a new hindered settling formula. New settling experiments on these highly concentrated suspensions are described to test this formula. For the analysis of the experiments both an analytical and a numerical method are used. Kynch's analytical theory, based on the method of characteristics is used to study the type of settling. Furthermore, a 1DV-point model is used for analysis of the settling process. We have implemented the new hindered settling formula in this model, which is tested against experimental data. It is concluded that the data are described fairly well. The analysis with the theory of Kynch [1952. A theory of sedimentation. Transactions of the Faraday Scociety 48, 166–176] and the model show that highly concentrated suspensions can settle with either one interface or with two interfaces, depending on the initial concentration and the shape of the settling flux function.
r 2007 Elsevier Ltd. All rights reserved.

PACS: 9999

Keywords: Kaolinite; Mud flocs; Cohesive sediment; Hindered settling

1. Introduction

In the past decades knowledge on the properties and behaviour of cohesive sediment has increased gradually, motivated by the awareness of the importance of cohesive sediments in the ecosystem, amongst other things. It was understood that cohesive sediment has important properties, such as its ability to adhere heavy minerals and other contaminants, and the fact that it may contain a high amount of organic material, a source of food for many organisms.

Much research has been carried out on the settling of low-concentration mud suspensions and on consolidation. Been (1980) and Sills (1997), amongst others, performed experiments on settling and consolidation of natural mud, and Merckelbach (2000) developed a consolidation model that was validated against experiments with natural mud. In contrast, little research has been published on the

ffiCorresponding author. Tel.: +31 243284601.
E-mail address: p.dankers@royalhaskoning.com (P.J.T. Dankers).

0278-4343/$ - see front matter r 2007 Elsevier Ltd. All rights reserved.
doi:10.1016/j.csr.2007.03.005

FOIA_07123_0005563_0001

settling behaviour of highly concentrated mud suspensions in general, and on the behaviour of highly concentrated mud–sand mixtures in particular. Yet, this is an important subject when studying, for instance, the transport and fate of dredging plumes and their effect on the ecosystem, and the siltation of navigation channels and harbour basins. The lack of proper understanding of hindered settling and its modelling is partly due to a lack of proper data.

In this paper, we report on the behaviour of highly concentrated mud suspensions only; mud–sand mixtures are treated in another paper. The goal of this research was to create a data set on the settling of highly concentrated mud suspensions, to describe and analyse their behaviour with Kynch's (1952) theory on hindered settling, and to develop a model for settling suspensions in the hindered settling regime. To reach this goal, experiments on highly concentrated cohesive sediment suspensions have been performed in the Environmental Fluid Mechanics Laboratory at Delft University of Technology. In this paper, we attempt to analyse the behaviour of these suspensions with the method of characteristics, a well known method for settling suspensions. Next, a 1DV model is used for further analysis of the experiments. The model consists of two parts, one for the mud fraction and the other for the sand fraction. Here, only the part of the model that describes the settling of highly concentrated mud suspensions is used.

2. Theories on hindered settling

2.1. Kynch's theory

A single particle or floc settling in still water has a specific settling velocity $(w_{s;0})$, which is a function of its shape, size, density and the viscosity of the fluid. When the concentration of particles increases, they start to interfere and hinder each other, thereby reducing their settling velocity. This is called hindered settling and the settling velocity is referred to as the effective settling velocity (w_s). When the concentration increases further, the particles tend to be in constant contact with each other, and a particle framework builds up. The change from a water supporting system to a sediment supporting system is called gelling and the gelling concentration (c_{gel}) is the concentration of the suspension at that point. Also, from this point early consolidation starts, water is squeezed out and effective stresses become measurable. Hindered settling of cohesive sediment flocs occurs when mass concentrations are larger than a few kg=m^3 (Mehta, 1986).

The theory of sedimentation of highly concentrated suspensions was first studied by Kynch (1952) and elaborated by, amongst others, Kranenburg (1992). Kynch (1952) introduced an empirical relationship between the effective settling velocity and the local sediment concentration (herein the local volumetric sediment concentration of the solids $f = c/c_{gel}$ is used), assuming that everywhere in the suspension the settling velocity of particles depends on the local concentration of particles only:

$$w_s = w_{s;0} f(f). \tag{1}$$

Here $w_{s;0}$ is the settling velocity of a single particle in still water in a Eulerian reference frame, positive downward, and $f(f)$ is a function that describes the effect of the concentration on the settling velocity, i.e., $f(0) = 1$ an $df(1) = 0$. Hence, the following 1-D vertical volume balance is derived:

$$\frac{\partial f}{\partial t} + w_{s;0} F'(f) \frac{\partial f}{\partial z} = 0, \tag{2}$$

where

$$F(f) = \frac{d}{df}\left[f f(f)\right] \tag{3}$$

and where t is time and z is the vertical coordinate, positive downwards. Eq. (2) is a 1-D simple wave equation, which is hyperbolic and its solution allows for the formation of shocks, also called interfaces. It can be solved by integrating along characteristic lines, i.e. lines of equal concentration (f), in the $(z; t)$ plane. These lines are given by

$$\frac{dz}{dt} = w_{s;o} F'(f) = C_c, \tag{4}$$

where C_c is the celerity (wave speed). The position of the characteristics in time t is given by

$$z(t) = z_0(f) + w_{s;0} F'(f) t, \tag{5}$$

where $z_0(f)$ represents the initial height of a specific concentration or characteristic. Two characteristic lines converge if dz/dz_0 decreases with time. Differentiating Eq. (5) gives

$$\frac{dz}{dz_0} = 1 + w_{s;0} \frac{dF}{df} \frac{df}{dz_0} t. \tag{6}$$

If the concentration increases with depth $(df/dz_0 > 0)$, and as an interface develops when characteristic paths converge, Eq. (6) implies that an interface in a settling suspension will develop when

FOIA_07123_0005563_0002

$dF/df > 0$. In still water there is always an interface between the water above the suspension and the settling suspension. A second interface, lower in the suspension, will occur when the above-mentioned criterion is met. As the upper interface is always present (in a mono-dispersed suspension) it can be concluded that when

$$\frac{dF}{df} > 0 \quad (7)$$

two interfaces develop and when

$$\frac{dF}{df} < 0 \quad (8)$$

only one interface develops. In the latter case, the concentration in the lower part of the suspension increases gradually. These two types of settling may both exist depending on the initial concentration. For suspensions that can settle in both modes there is a concentration, f_{cr}, at which the behaviour changes from settling with two interfaces to settling with one interface. It is obvious that any hindered settling model must account for this behaviour.

Thus, we conclude that the interference between characteristics can result in a jump in concentration (interface) or a gradual change in concentration. A jump is called a regular shock or a compound shock wave. It occurs when the characteristic lines cross from both sides (Fig. 1a and b) (Bartholomeeusen et al., 2003). A gradual change, in which the characteristics diverge, is called a rarefaction wave (Fig. 1c).

The upper interface generally consists of a regular shock wave. In the suspension itself all three types of waves are theoretically possible. A regular or compound shock wave occurs when $dF/df > 0$, and a rarefaction wave when $dF/df < 0$. A regular shock wave is, however, highly unlikely (Bustos et al., 1999). In experimental situations when a lower interface is present, there is a gradual increase from the shock towards the gelling concentration (Toorman, 1992), indicating a compound shock wave.

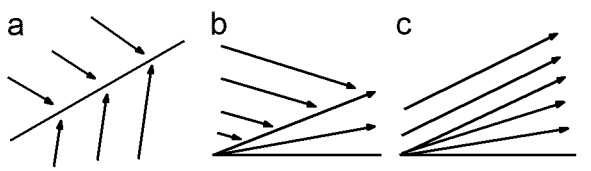

Fig. 1. Three possible types of characteristic wave paths. (a) Regular type; (b) compound type; and (c) rarefaction type (after Bartholomeeusen et al., 2003).

Whether compound, regular or rarefaction waves occur depends on the flux function (Sf) and the position of the initial volumetric concentration on the flux function. Bartholomeeusen et al. (2003) and Bustos et al. (1999) show that the speed of the shock wave, s, is determined by the Rankine Hugoniot jump condition:

$$s = \frac{S(f_u) - S(f_d)}{f_u - f_d} \quad (9)$$

and that a regular or compound shock occurs when Oleinik's jump entropy condition is fulfilled (Bustos et al., 1999):

$$\frac{S(f) - S(f_u)}{f - f_u} \geq s \geq \frac{S(f) - S(f_d)}{f - f_d}$$

or

$$w_{s;0}(f_u) \geq s \geq w_{s;0}(f_d) \quad (10)$$

with f_u and f_d the volumetric concentrations just above and just below the shock, respectively. When Eq. (10) is not fulfilled there will be a gradual transition of concentration (rarefaction wave, Fig. 1c).

2.2. From theory to application

The ultimate purpose of this study is to derive a formulation for the settling behaviour of sediment in complex 3D models. For this purpose, an ''integral'' advection–diffusion equation was derived (Winterwerp and Van Kesteren, 2004) that accounts for both the (hindered) settling and consolidation regimes and which can be applied from the water surface into the bed. This advection–diffusion equation for the hindered settling and consolidation of a suspension reads

$$\frac{\partial f_p}{\partial t} = \frac{\partial}{\partial z}(X_s f_p) + \frac{\partial}{\partial z}\left[(D_s + G_T + G_c)\frac{\partial f_p}{\partial z}\right], \quad (11)$$

where $f_p(= c/\rho_s)$ is the volumetric primary particle concentration of the solids fraction, X_s is the settling function (Winterwerp and Van Kesteren, 2004), D_s is the molecular diffusion coefficient, G_c is the diffusion component (i.e. consolidation coefficient) in the consolidation formula in which fractal theory has been used, and G_T is the eddy diffusivity. The advection–diffusion equation can be rewritten as

$$\frac{\partial f_p}{\partial t} = \frac{\partial}{\partial z}\left[X_s f_p + (D_s + G_T + G_c)\frac{\partial f_p}{\partial z}\right]. \quad (12)$$

FOIA_07123_0005563_0003

The settling function in the advection term consists of two parts:

$$X_s = w_s + \frac{f_c}{1 + Zf_c} \tag{13}$$

in which the first term is the advective particle flux in the hindered settling regime and the second term the advective particle flux in the consolidation regime, with w_s is the effective settling velocity, Z is a heuristic parameter to obtain a smooth transition between the descriptions for hindered settling and permeability and

$$f_c = \frac{r_s - r_w}{r_w} k f_p \tag{14}$$

with r_s is the solids density, r_w is the density of water and k is the permeability.

The diffusion term, G_c, in Eq. (12) describes consolidation when the effects of effective stress and permeability are dominant, while the consolidation part, f_c, in the advection term describes early consolidation when the effect of permeability only is dominant. The flux in Eq. (12) can thus be divided into three phases, namely a hindered settling phase, a phase where the effects of permeability are dominant and a phase where the effects of effective stress are dominant. The latter two comprise consolidation. Of course, these regimes may overlap partly. A similar kind of division is made by Lester et al. (2005).

The complete advection–diffusion equation cannot be solved with Kynch's method. However, when the diffusion term in Eq. (12) is small, only the settling function is left, and the equation reduces to the simple wave equation which can be solved with the method of characteristics. The first stage of consolidation, where permeability effects are important, is still incorporated in this equation and can thus be resolved, c.q. analysed, with this same method of characteristics that was described in the previous section.

Fig. 2 shows a sketch of the complete flux function of Eq. (12), which contains an advection part and a diffusion part. The advective part is governed by hindered settling and the effects of permeability, whereas the diffusive part is governed by the effects of permeability and effective stresses. The hindered settling part ends at $f_{p;gel}$ where the flux, if we only account for the hindered settling flux, is 0. The definition of $f_{p;gel}$, used in this study, comprises nothing more than at that concentration the hindered settling function yields $w_s = 0$. By

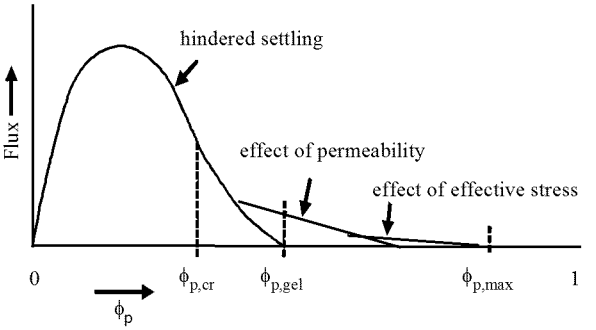

Fig. 2. A sketch of the flux in Eq. (12) as a function of f_p. Three processes are incorporated in the flux: hindered settling, the effect of permeability and the effect of effective stress. For clarity, the joint effect of effective stress and permeability, as modelled in the diffusion term, is referred to as the effect of effective stress only.

incorporating the effects of consolidation (both permeability and effective stress), the settling flux reduces slower, becoming 0 at $f_{p;max}$ only. At this concentration, the sediment load is completely supported by internal stresses. Yet, some further compaction is possible because of creep. f_{cr} depicts the (first) inflexion point of the flux function and indicates the change between settling with two interfaces to settling with one interface.

Permeability effects start to become important around $f_{p;gel}$. This implies the existence of five stages: a hindered settling stage, a stage where hindered settling overlaps with the effects of permeability, a stage where permeability effects are dominant, a stage where the effects of permeability overlap with the effects of effective stress and a stage where effective stress is dominant (Fig. 2). The latter three cases comprise consolidation. The second stage, where hindered settling and permeability effects during early consolidation are important is referred to as the ''fluid mud phase'' (we realise that this is not a common definition for fluid mud). In our theory, hindered settling takes place in this area as $f_p \approx f_{p;gel}$. In reality, the effects of permeability influence the settling behaviour when f_p approaches $f_{p;gel}$ and Darcy's law becomes relevant.

As said, we define the transition from the hindered settling phase to the consolidation phase with $f_{p;gel}$. We appreciate that effective stresses may develop at $f_p \approx f_{p;gel}$. However, it can be shown (Winterwerp and Van Kesteren, 2004) that at $f_{p;gel}$, the effective stress $\sigma' \approx 1$ Pa, which amounts to a few tenth promille of the total stress in the bed. Therefore, we distinguish between f_{gel}, which marks

FOIA_07123_0005563_0004

the artificial transition between hindered settling and consolidation, and f_{struc}, which marks the onset of a (measurable) effective stress.

These five separate stages and three phases are shown again in Fig. 3 in a log–log plot of the complete settling flux against volumetric particle concentration, based on data presented in Winterwerp and Van Kesteren (2004). It shows a stage with hindered settling, followed and overlapped by a stage of early consolidation where permeability is important, followed and overlapped by a stage of consolidation where the effect of effective stress is important, followed by a stage where only effective stress is important.

The types of sedimentation with the definitions that will be used in this study are shown in Fig. 4.

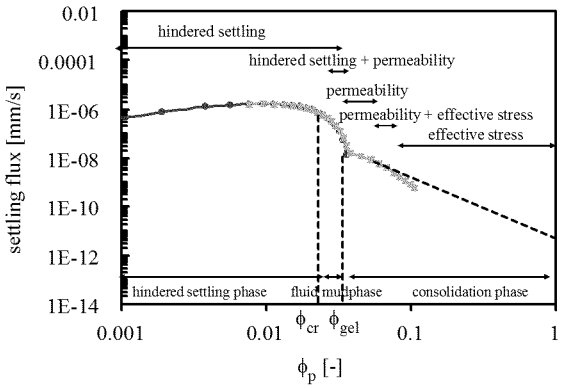

Fig. 3. Double logarithmic plot of the settling flux against f_p.

In this study all equations are related to the volumetric floc concentration ðf ¼ c=c_{gel}Þ instead of f_p, and we define f ¼ 1 at c_{gel}, implying that f can become larger than unity when consolidation takes place. Instead of the often used structural density r_{struc} we choose to use c_{gel} as the division between hindered settling and consolidation, as reasoned above.

In the top panel of Fig. 4, the initial concentration f_i o f_{cr} and dF=d f o 0, which means there are two interfaces. These interfaces are indicated by the converging characteristics. The upper interface is a regular shock, while the lower interface is a compound shock (Fig. 1a and b), later followed by a rarefaction wave. As explained before, we refer to the area above the compound shock as the hindered settling phase, below, at f o 1 as ''fluid mud phase'', and for f 4 1 as the consolidation phase. Hindered settling takes place in the hindered settling and in the ''fluid mud phase''.

In the lower panel, f_{cr} o f_i o f_{gel} and the characteristic lines intersect with each other to form an upper interface (regular shock). In the suspension itself the characteristics do not intersect and a rarefaction wave is formed (Fig. 1c). Within the area in which the characteristic lines are parallel to each other hindered settling takes place. Lower in the suspension the concentration increases gradually, which is indicated by the diverging characteristics. This is the start of the ''fluid mud phase'', which changes to the consolidation phase when the

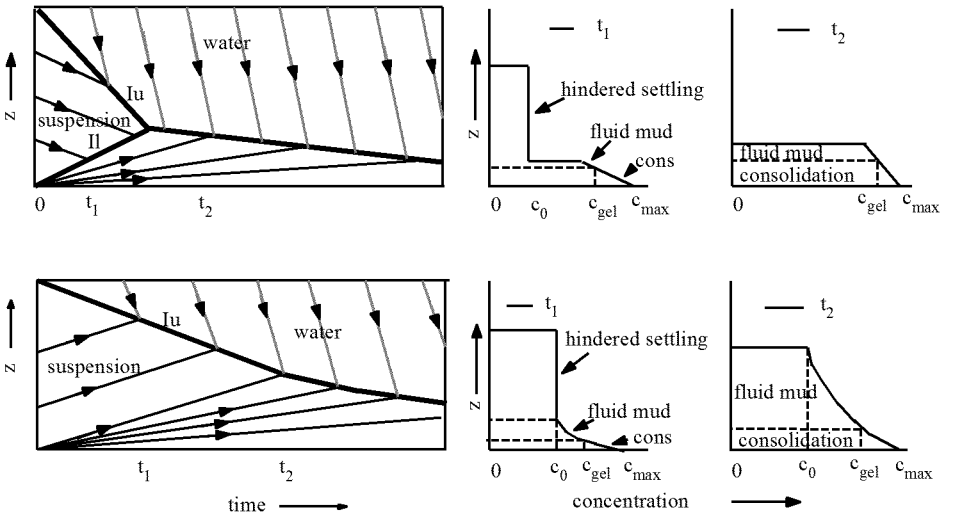

Fig. 4. Two different settling behaviours for uniform initial concentration distributions according to Kynch. Characteristic lines (marked with arrows), interfaces (Iu ¼ upper interface, Il ¼ lower interface) and concentration distributions at two time levels. Adapted from Kranenburg (1992).

FOIA_07123_0005563_0005

concentration becomes larger than the gelling concentration.

This theory is used to analyse the experimental data. Furthermore, we develop a model that accounts for the above-described theory by allowing both types of settling.

2.3. Hindered settling function

The hindered settling function $f(f_p)$ in Eq. (3) needs to be specified. By applying the above theory we examine the settling behaviour predicted by different hindered settling functions. Commonly, the well known hindered settling equation by Richardson and Zaki (1954), adjusted for cohesive sediment flocs by Mehta (1986), is used:

$$w_s = w_{s;0}(1 - k f_p)^n, \tag{15}$$

where k is an empirical parameter, f_p is the volumetric concentration of the solids, $f_p = c/\rho_s$ in which c is the mass concentration and ρ_s the density of the sediment, and n is a function of the particle Reynolds number. Many studies on hindered settling of sand, discussed briefly in a paper by Mandersloot et al. (1986), make use of this model.

In Winterwerp (2002) and Winterwerp and Van Kesteren (2004) this model is reanalysed. Winterwerp (2002) used the same rationale as Mandersloot et al. (1986) and Scott (1984) for the analysis of the hindered settling of cohesive sediment and cohesive sediment mixtures. He reasons that, as each floc within a suspension can be considered to settle in the remainder of the suspension, this would result in three hindering effects:

- Return flow and wake formation: Settling particles generate a return flow and a wake. Neighbouring particles will be influenced by this effect and their effective settling velocity will be decreased by a factor $(1 - f)$, where $f = c/c_{gel}$ is the volumetric concentration of flocs.
- Viscosity: Each floc settles in the remainder of that suspension which has an increased viscosity. As no proper formulations exist for the viscosity in the range of mud concentrations treated in this paper, we use the classical formula of Einstein, i.e. $\mu_{eff} = \mu_{mol}(1 + 2.5f)$ in which μ_{eff} is the effective viscosity and μ_{mol} is the molecular viscosity.
- Buoyancy or reduced gravity: Invoking the same argument, flocs settle in a suspension with an increased bulk density. The effective settling velocity is decreased by a factor $(1 - f_p)$, where $f_p = c/\rho_s = c_{gel} f/\rho_s$ = the volumetric concentration of the solids.

This reasoning led to a new formula for the hindered settling of mud flocs:

$$w_s = w_{s;0}\frac{(1 - f)^m(1 - f_p)}{1 + 2.5f}. \tag{16}$$

The exponent m accounts for possible non-linear effects. When the return flow effect is linear ($m = 1$), only the volume effect of sediment settling in a liquid is taken into account. The downward flux of sediment creates an equal upward flux of water (with sediment) when non-linearity is taken into account ($m > 1$). This means that hydrodynamic effects generated by the settling particle (for example acceleration and deceleration of flow, and the curvature of streamlines) are incorporated.

The behaviour of these equations, and especially the occurrence of a minimum in F (Eq. (3)), determines if and when shock waves occur. For both Eqs. (15) and (16), f decreases monotonically with f (Fig. 5). The function F, however, behaves differently. In the case of Eq. (15), with $n = 4$, F has a minimum at a volumetric concentration f_{cr}. This concentration indicates a change in the sign of dF/df (Eqs. (7) and (8)), and thus, a change from the occurrence of two interfaces to one interface. The function F in Eq. (16) shows different profiles depending on the choice of m, an empirical parameter that cannot be quantified analytically. For $m = 1$, F decreases monotonically with f, but

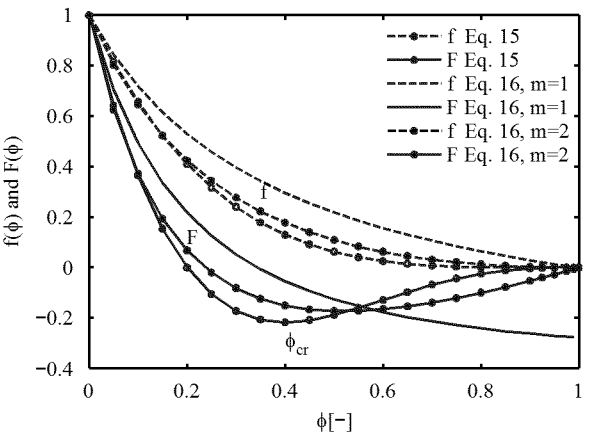

Fig. 5. Variation of hindered settling functions f and F for Eq. (15) ($k = 1$, $n = 4$) and Eq. (16) ($m = 1$ and $m = 2$). For c_{gel} a value of 85 kg/m^3 is used. Based on Kranenburg (1992) and Winterwerp (2002).

FOIA_07123_0005563_0006

for $m \neq 1$, F shows a minimum. The non-linear effects in the return flow lead to the occurrence of two or one interfaces depending on the initial conditions, while a linear return flow will always generate two interfaces. The value of m can be determined when f_{cr} is known. F is given by

$$F(f) = \left[\frac{d}{df}(f f(f))\right]_{cr} = \frac{(1-f)^m(1-c_{gel} f/r_s)}{1+2.5f} - f\frac{(1-f)^m m(1-c_{gel} f/r_s)}{(1-f)(1+2.5f)} - f\frac{(1-f)^m c_{gel}}{r(1+2.5f)} - 2.5f\frac{(1-f)^m(1-c_{gel} f/r_s)}{(1+2.5f)^2}. \quad (17)$$

From $dF/df = 0$ at $f = f_{cr}$, m is obtained as

$$m = \frac{1}{2}\frac{5f_{cr}^2 - 2f_{cr} + 4 + \sqrt{25f_{cr}^4 + 60f_{cr}^3 - 116f_{cr}^2 + 64f_{cr} + 16}}{f_{cr}(2+5f_{cr})}. \quad (18)$$

In the next sections Eq. (16) is validated against experimental data. The parameters needed for the model have been derived previously (Dankers et al., 2007), but their derivation is given briefly in the next section.

3. Experiments

3.1. Experimental setup and methodology

Settling experiments were performed in the laboratory of the Environmental Fluid Mechanics Section at Delft University of Technology, using acrylic columns with heights of 40 cm and a diameter of 7 cm. The suspensions were prepared with kaolinite, a clay mineral with low cohesive properties. All 16 experiments were conducted using different initial concentrations. The goal was to create a data set for the calibration and validation of the hindered settling model (Eq. (16)). The parameters to be determined are the gelling concentration (c_{gel}), the parameter m and $w_{s;0}$, the settling velocity of a single kaolinite floc in still water. The suspension was prepared by adding salt water ($\rho = 1003\ kg/m^3$) to kaolinite powder. This suspension was then stirred thoroughly for at least two weeks in order for a steady chemical state to develop. The 16 experiments were carried out in two series. The second series was performed two months after the first, using the same initially prepared mixture. In each experiment a sample was taken from the tank and diluted with salt water to the desired initial concentration, whereafter it was poured in one of the settling columns, mixed and allowed to settle.

The settling of the upper interface, which is the interface between clear water and the suspension, was monitored visually. Furthermore, concentration time series were measured at three or four different heights in the column. This was done with a conductivity probe (measuring resolution is $\pm 2\ kg/m^3$), developed by WLjDelft Hydraulics. An Anton Paar meter was used to measure suspension density.

3.2. Results

3.2.1. Settling curves

For all the 16 experiments the effective settling velocity of the suspension is determined where possible, by taking the tangent of the settling curves, all of which are shown in Fig. 6.

Kynch (1952) described two types of settling curves (Fig. 4) that are recognised in Fig. 6 as well. The first type of settling curve in Fig. 4 is characterised by a profile with a steep hindered settling part and a less steep consolidation part. In Fig. 6 the curves with initial concentrations up to $50\ kg/m^3$ show this kind of behaviour. The upper interface in these cases is represented by the actual settling curve, while the lower interface is represented by the imaginary line from the origin to the

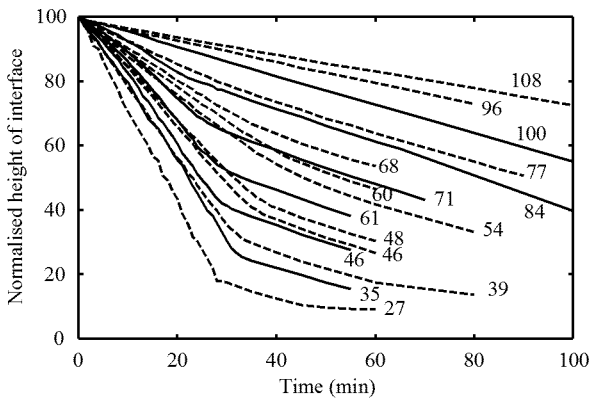

Fig. 6. Normalised settling curves for different kaolinite concentrations. Solid lines represent Series 1 and dashed lines represent Series 2. Numbers indicate initial concentration (kg/m^3). The initial height was varied between 34 and 37 cm.

FOIA_07123_0005563_0007

point of contraction (see also Fig. 4). The second type of settling curve is characterised by a gently sloping curved line. This type has only one interface, the upper interface, and according to the curves in Fig. 6 this behaviour occurs when the initial concentration is larger than 60 kg=m^3. In the latter case, there is either a short hindered settling and fluid mud phase followed by consolidation $\delta f_{cr} < f_i < f_{gel}\beta$, or consolidation from the start $\delta f_i > f_{gel}\beta$.

Although the consolidation phase is present in Fig. 6, only the part of the curve representing hindered settling is examined.

3.2.2. Gelling concentration

The gelling concentration is difficult to assess accurately. Therefore, we use two methods for its derivation. Often, the gelling concentration is determined from a mass balance of the settling sediment and the average concentrations above and below the lower interface. This method gives an approximation of the gelling concentration as it only gives accurate results when there is no consolidation. When consolidation occurs the gelling concentration is overpredicted. To determine the gelling concentration with this method we use

$$hc_i = \int_0^{h\delta t\beta} c\,dz = \int_0^{d_1} c\,dz + \int_{d_1}^{h} c\,dz \approx c_{gel} d_1 + c_2 d_2 \tag{19}$$

leading to

$$c_{gel} = \frac{c_i h - c_2 d_2}{d_1} \tag{20}$$

in which c_i is the initial mass concentration, h is the initial height, c_2 is the concentration in the zone from the first interface to the shock or second interface (see also Fig. 4 in which $c_2 = c_i$), d_2 is the height from the upper interface to the lower interface at time t, and d_1 is the thickness of the ''bed'' (from the lower interface to the bottom of the column at time t). This means that the calculated c_{gel} is approximated by the average concentration over d_1. In Fig. 4, top panel, it can be seen that the characteristic lines in that area form a fan and the concentration increases towards the bed. Using this method for all experiments we obtain $c_{gel} = 109 - 8$ kg=m^3. The actual value of c_{gel} will be lower, as the concentration of the suspension in layer d_1 is affected by consolidation.

A second method to obtain c_{gel} is to use measured concentration profiles. A conductivity meter placed a few centimetres above the bottom of the column was used for this purpose. Some of the concentration time series measured in our experiments are shown in Fig. 7. In these profiles the concentration increases gradually with time until the gelling concentration is reached (boxed area in Fig. 7). At this point the mud flocs are close enough to provide structural support and consolidation, which is a slow process, begins.

In this way the gelling concentration was obtained from the bed level measurements with the conductivity meter. This was done for most of the experiments, except for the ones in which the initial concentration was larger than the gelling concentration, or for a few experiments in which the conductivity probe was placed too high.

The gelling concentrations determined with the conductivity probe are shown in Fig. 8. A trend of increasing gelling concentrations for increasing initial concentrations is visible. At first glance this is remarkable, as higher initial concentrations result in larger flocs, hence lower gelling concentrations would be expected. However, larger flocs break up more easily and this anomalous behaviour may be explained by other factors that influence the floc size and thus the gelling concentration, such as flow effects (shear), the type of sediment, the type of environment (e.g. salt water or the availability of organic material) and most importantly the stress history. Fig. 8 shows that the gelling concentration is not a constant. However, our final goal is to

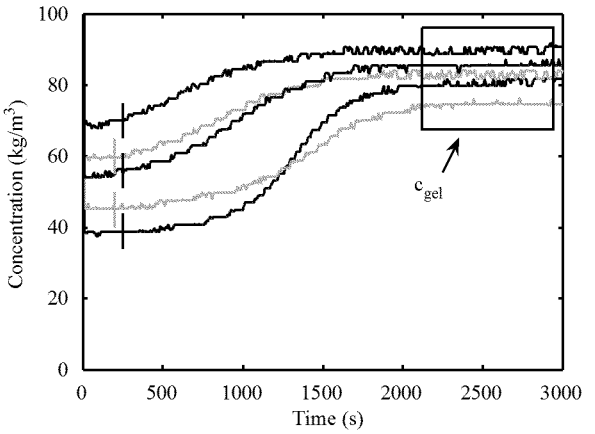

Fig. 7. Concentration–time series for experiments with different initial concentrations. At t = 2000s from top to bottom: c_i = 68; 54; 60; 39; 48 kg=m^3; vertical lines represent estimated experimental error.

FOIA_07123_0005563_0008

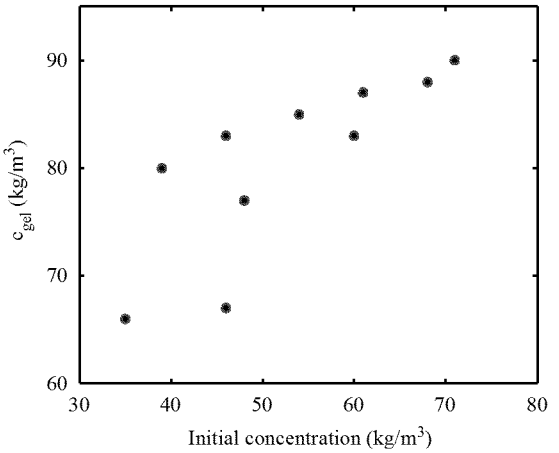

Fig. 8. Measured gelling concentrations.

model the settling behaviour. For predictability it is more convenient to use a mean constant gelling concentration. In this study, the mean gelling concentration that was derived with the second method (c_{gel} ¼ 81 – 8 kg/m^3) is used. The maximum and minimum gelling concentrations can be used to determine the sensitivity of the model results to c_{gel}. For more advanced modelling, the gelling concentration can be made dependent on the floc size. The latter is beyond the scope of this study.

The accuracy of the conductivity meter depends on temperature and it is quite sensitive to vibrations, air bubbles and clogging. An advantage, however, is that the initial concentrations are known exactly and the slope of the calibration profile is almost the same for all the measurements within one experiment. Therefore, the actual error in the density measurements is estimated at about – 5 kg/m^3.

A summary of all the experimental results is given in Table 1.

Table 1
All experiments with their initial concentration, effective settling velocity and gelling concentration

Id	c_i (kg/m^3)	w_s (mm/s)	c_{gel} (kg/m^3)
30kol	35	0.134	66
40kol	46	0.111	83
50kol	61	0.071	87
60kol	71	0.058	90
70kol	84	0.052	—
80kol	100	0.028	—
10tt	27	0.170	—
20tt	39	0.133	80
30tt	46	0.101	67
40tt	48	0.096	77
50tt	68	0.067	88
55tt	54	0.075	85
60tt	77	0.059	—
70tt	60	0.044	83
80tt	96	0.022	—
90tt	108	0.019	—

3.2.3. Characteristics and non-linear effects

We analysed the experiments using the method of characteristics to see whether shocks occurred. In Fig. 9 two settling curves are shown with their characteristics based on experimental results. The conductivity meter was used to determine the concentration at four different heights in the suspension. Fig. 9a clearly shows two interfaces. The upper interface is represented by the dot-dashed line, while a lower interface is found where the characteristic lines converge. Near the upper interface the concentration decreases somewhat. This might be due to segregation, diffusion and/or wall effects. For mono-dispersed suspensions, in which no segregation occurs, the concentration in this zone should be equal to its initial value. In that case, characteristics cannot be obtained experimentally, but the direction of propagation of the characteristics can be derived mathematically by taking the tangent of the flux function (S). The direction of characteristics in the hindered settling phase is therefore more an indication of trend as their direction is not always unambiguous. Beneath the lower interface only one data point per characteristic is available. This means that the characteristics in this area do not completely arise from empirical observation but that their direction is derived on the basis of both empirical observation and expected behaviour. First, $c \circ c_{gel}$ and a fluid mud phase develops, which changes to consolidation when $c 4 c_{gel}$.

Fig. 9b has a different appearance. There are no converging characteristics, which means that there is no shock or lower interface in the suspension. The characteristics have a fan-like configuration, indicating a rarefaction wave. Because we are dealing with a rarefaction wave we have:

| hindered settling with one interface ($f 4 f_{cr}$), or
| consolidation ($f 4 1$, $c_i 4 c_{gel}$)

In this experiment c_i ¼ 61 kg/m^3, which means that the first is true as c_{gel} ¼ 81 kg/m^3.

FOIA_07123_0005563_0009

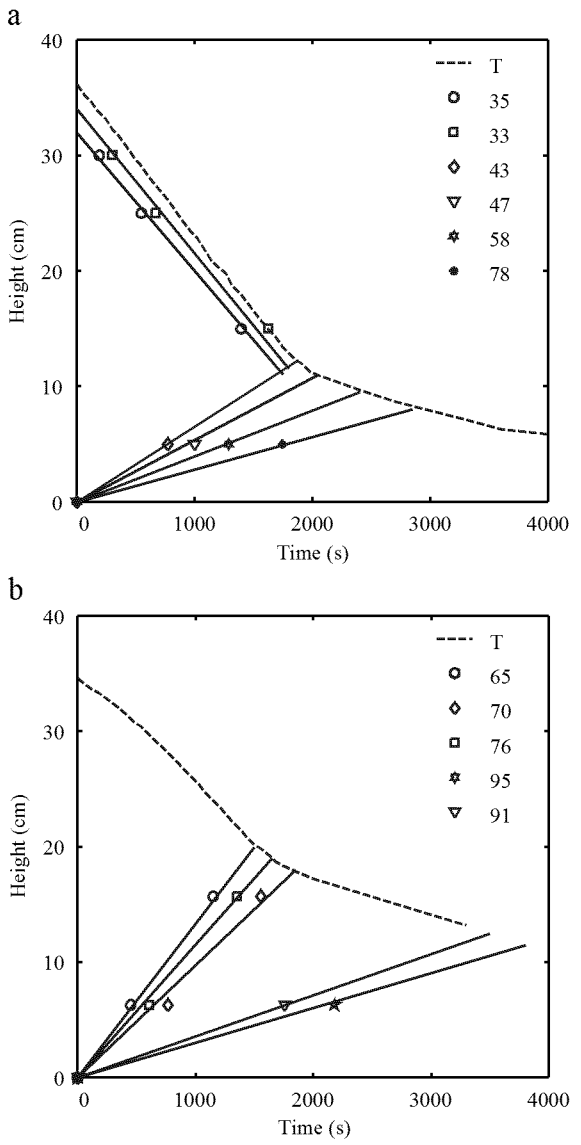

Fig. 9. Settling curves from experiment 20tt ðc_i ¼ 39 kg=m³Þ and 50kol ðc_i ¼ 61 kg=m³Þ with characteristic lines.

From the above analysis we can conclude that there can be a compound shock wave within the suspension, the so-called lower interface, if $c_i < c_{gel}$, and a rarefaction wave if there is no lower interface. Other indications confirming that there can be only one upper interface and no lower interface are given in Dankers et al. (2007). This means that, according to the theory of Section 2.1, the flux function F should fulfill both Eqs. (7) and (8). In that case the flux function has a minimum at f_{cr}, as shown in Fig. 5. In Eq. (16) this is only true when non-linearities in the return flow effect are incorporated (i.e. m41). In Dankers et al. (2007) a value of $0{:}43 < f_{cr} < 0{:}68$ was found which gives $m \geq 2$ from Eq. (18).This value will be used in the modelling experiments.

4. 1DV modelling

Next, the hindered settling equation (16), incorporated in the 1DV point model by Delft Hydraulics, is used for a further analysis of hindered settling. The simple wave equation (Eq. (2)) describes the hindered settling regime, but not the consolidation regime as the equation becomes parabolic when effective stresses occur (Winterwerp and Van Kesteren, 2004). Moreover, the simple wave equation describes hindered settling in still water only, as in flowing water (turbulent) diffusion must also be accounted for. Therefore, hindered settling, turbulent diffusion and consolidation have all been incorporated in the advection–diffusion equation implemented in the 1DV-point model. This implies that this model is not fully suited to solve the simple wave equation. However, if diffusion is small, as is the case with molecular diffusion, the model results should be accurate enough. This assumption is elaborated upon next.

4.1. Model description

The 1DV model was developed on the basis of DELFT3D-FLOW by stripping all horizontal gradients except the horizontal pressure gradient. It is described in Winterwerp (2002) and Uittenbogaard et al. (1996). The vertical transport of sediment is modelled with the advection–diffusion Eq. (12).

The equations are solved using a staggered grid, consisting of 100 layers in the vertical. A first order upwind scheme is used together with a three-point scheme for the diffusion operator in vertical direction. A time step of 1 s or 1 min is used. The numerical diffusivity (D_{num}) for the upwind scheme amounts to $D_{num} = w_s Dz/2 \geq ð0{:}3 - 3Þ \bullet 10^{-7}\ m^2/s$ (Winterwerp and Van Kesteren, 2004). In our case, the particle diffusion is set to $D_s = 5 \bullet 10^{-8}\ m^2/s$. It follows from $w_s \geq 10^{-4}$ m/s and $D_s/Dz \geq 10^{-6}$ m/s, that $w_s \gg D_s/Dz$ and diffusion is negligible. Only at the end of the hindered settling phase, where the settling velocity approaches zero, numerical diffusion may start to play a role. The parameter settings were derived from the experiments and are explained next.

FOIA_07123_0005563_0010

4.2. Calibration

The input parameters for the model are the initial concentration distribution, the gelling concentration $\delta c_{gel}\Phi$, the settling velocity of single flocs $\delta w_{s;0}\Phi$ and the non-linearity parameter (m). For the gelling concentration we use the mean gelling concentration from Table 1, which is 81 kg=m^3. It is understood that the gelling concentration is not constant, but lies within a certain range, depending largely on history effects, type of minerals, chemistry of pore water, organic components (EPS, TEP), etc. For modelling purposes these effects cannot be incorporated easily and a mean gelling concentration is therefore used. The factor m is set to 2, e.g. Dankers et al. (2007). This means that non-linearities in return flow are taken into account, and the formation of a second interface is allowed. It is not possible to derive the parameter $w_{s;0}$ from measurement directly. With kaolinite suspensions it is impossible to distinguish single particles, as the whole suspension is milky, even at low kaolinite concentrations. Therefore, the value of $w_{s;0}$ is derived from fitting model results to the results of a few experiments. The $w_{s;0}$ values are expected to change with initial concentration, as larger flocs will be formed with increasing initial concentrations.

From Fig. 10a a settling velocity for single flocs of $0{:}7 \bullet 10^{-3}$ m=s is obtained, while Fig. 10b gives a best fit with $1{:}5 \bullet 10^{-3}$ m=s.

A good fit is obtained in the hindered settling regime of the two data sets. However, when the consolidation phase is reached the model does not fit the experiments, which is due to the fact that consolidation is not incorporated in the model. In the hindered settling model, the bed concentration cannot exceed c_{gel}, whereas in the experiments the concentration could be larger than c_{gel} because of consolidation. Hence, the interface could become lower in the experiments.

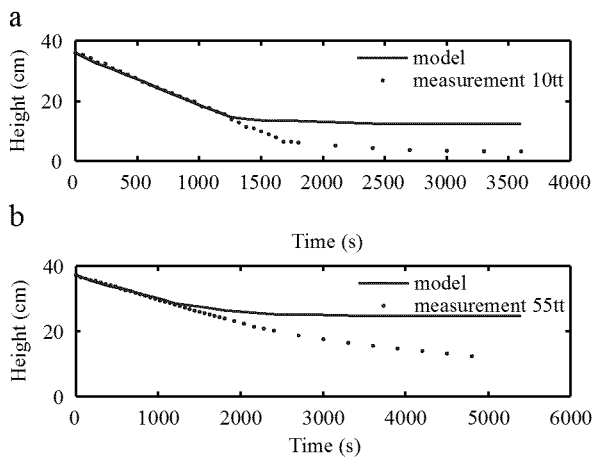

Fig. 10. Model fit to experiments 10tt δc_i ¼ 27 kg=m$^3\Phi$ and 55tt δc_i ¼ 54 kg=m$^3\Phi$ to establish $w_{s;0}$.

4.3. Results

After the model is calibrated for experiment 10tt and 55tt, a validation with the other experiments is performed. The value of $w_{s;0}$ for the other experiments is obtained through linear interpolation and extrapolation against the initial concentration of the values obtained for experiment 10tt and 55tt (Table 2). This means that $w_{s;0}$ is not a completely independent parameter. For both c_{gel} and m, the mean value that was derived from the experiments is used, hence also these parameters are not completely independent.

Thus, all parameters are now set to model the hindered settling behaviour. Three examples are presented in Fig. 11.

Fig. 11a–c show good results in the hindered settling regime but a deviation is observed of the model result in and just before the consolidation regime. In general, the higher the initial concentration the sooner this deviation occurs.

All modelling results are summarised and compared with experimental results in Fig. 12.

Table 2
Settling velocity of a single particle in still water for different initial concentrations

Id	c_i δkg=m$^3\Phi$	$w_{s;0}$ (mm/s)
30kol	35	0.95
40kol	46	1.28
50kol	61	1.73
60kol	71	2.03
70kol	84	2.42
80kol	100	2.90
10tt	27	0.71
20tt	39	1.07
30tt	46	1.28
40tt	48	1.34
50tt	68	1.94
55tt	54	1.52
60tt	77	2.21
70tt	60	1.70
80tt	96	2.78
90tt	108	3.14

FOIA_07123_0005563_0011

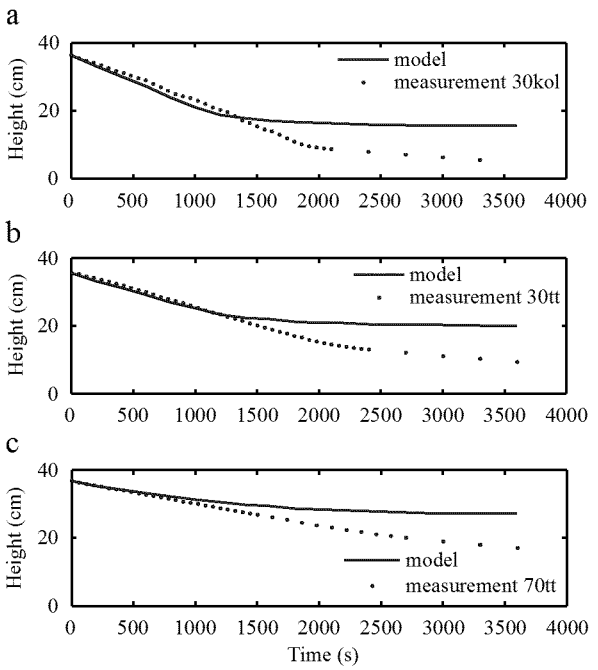

Fig. 11. Validation of the calibrated model with experiments 30kol (c_i = 35 kg/m^3), 30tt (c_i = 46 kg/m^3) and 70tt (c_i = 60 kg/m^3).

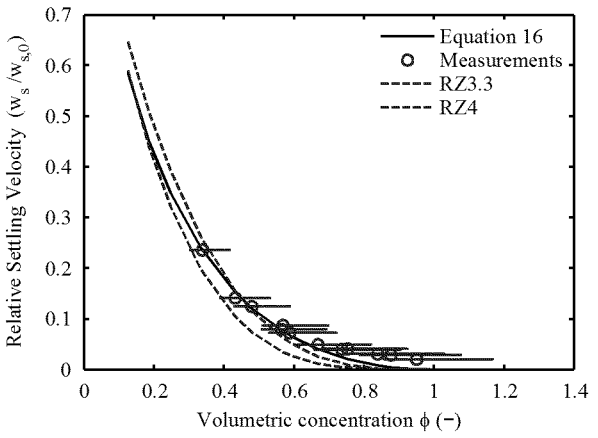

Fig. 12. Relative settling velocity obtained from experimental results compared with Eq. (16) with m = 2 and Eq. (15) (RZ) with n = 3.3 and 4.

Eq. (16) gives good results for low initial volumetric concentrations, (f_i < 0.7 or c_i < 60 kg/m^3). At higher concentrations the computed settling velocities are slightly lower than the measured ones as a result of consolidation. The experimental results are also compared with the Richardson and Zaki (1954)

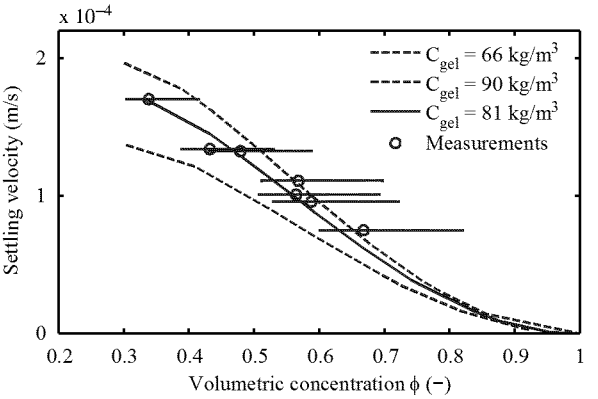

Fig. 13. Sensitivity of the model to gelling concentration. Lines show model fit with c_{gel} = 66, 81 and 90 kg/m^3.

formula, Eq. (15). First, n is set to 4, as recommended by Mehta (1986). This results in an underestimation of the effective settling velocity. By fitting the model to the data, we find a value of n = 3.3 to be more appropriate, comparable to Eq. (16). The measurements are presented together with their error bands. These bands indicate the range of volumetric concentrations if not the mean c_{gel} = 81 kg/m^3, but the minimum c_{gel} = 66 kg/m^3 and maximum c_{gel} = 90 kg/m^3 are used to calculate the volumetric concentration from the mass concentration.

The sensitivity of the model to the gelling concentration is shown in Fig. 13, where the minimum and maximum values for c_{gel} are used, while all other parameters are kept constant.

This figure shows the bandwidth within which the model results can vary when another gelling concentration is chosen. Only experiments with f_i > 0.7 are shown. Fig. 13 shows that both the mean and the maximum values of c_{gel} describe the data properly, the latter in particular at larger initial concentrations. For c_{gel} = 66 kg/m^3 there is a considerable deviation from the data.

Next, we analyse the concentration time series of measurements. In Fig. 14 the concentration time series are shown for several experiments. This figure shows whether the model predicts the proper velocity of the interface, and whether the measured jump in concentration across the interface is accurately modelled. Grey lines represent the model results, showing a fair agreement with data. It is noted that the computed interfaces do not appear as thin shocks, but have a certain thickness over which the concentration increases.

FOIA_07123_0005563_0012

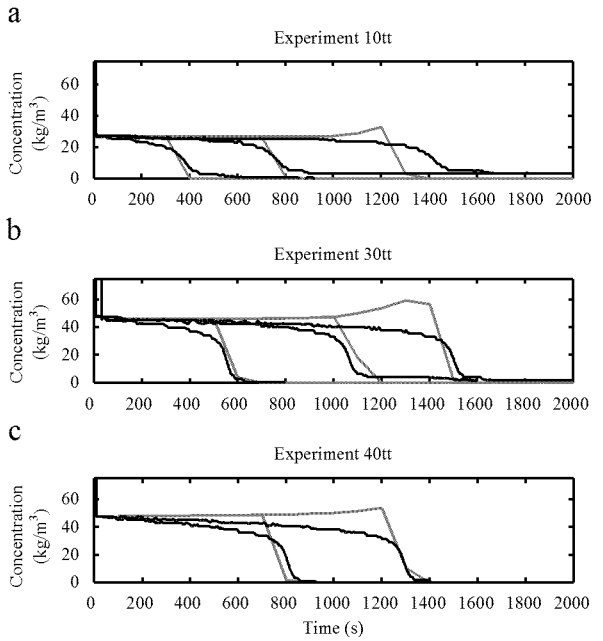

Fig. 14. Comparison of model (grey lines) and experiments (black lines) for concentration time series. (a) Experiment 10tt $\delta c_i \approx 27\ kg/m^3$ at 30, 23 and 15 cm above the column bottom. (b) Experiment 30tt $\delta c_i \approx 46\ kg/m^3$ at 30, 25 and 23 cm above the column bottom. (c) Experiment 40tt $\delta c_i \approx 48\ kg/m^3$ at 29 and 25 cm above the column bottom.

This is due to some (numerical) diffusion in the 1DV model.

The concentration distribution computed at the lowest measuring point shows a small overshoot, which is due to numerical effects. The gradual decrease in the measured concentration across the interfaces is due to the measuring volume of the instrument and its limited response time and possibly also due to some segregation of mud flocs in the top layer.

The error in the experimental data is estimated within $\pm 5\ kg/m^3$, e.g. the error band in Fig. 7.

Finally, we investigate the sensitivity of the model to variations in m, as its actual value lies in the range of 1:4 o m o 2:6. This parameter may change in value for different clay minerals or in case the samples have a different stress history. The lower value of m shows a better agreement at high f, whereas at lower f, $m \approx 2$ gives a better agreement with the data (Fig. 15). The sensitivity is not very high, as long as $m \geq 1$, as for $m \approx 1$ the behaviour of the settling curve changes.

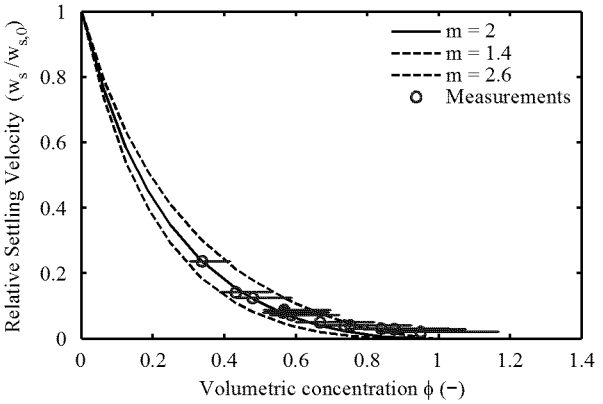

Fig. 15. Comparison between model results and data for $m \approx 2$, 2.9 and 1.4.

5. Summary and conclusions

This paper deals with the hindered settling of mud flocs. Experiments are described and analysed analytically with Kynch's theory of a settling suspension, using the simple wave equation to predict shocks within the suspensions. Furthermore, a numerical analysis is performed using a 1DV model in which that uses an advection–diffusion equation is implemented with a continuous description of hindered settling and consolidation. The 1DV model makes use of a hindered settling formula, which is validated against experimental data.

The analytical approach, in which hindered settling is analysed with the method of characteristics, showed that there are two types of settling, depending on the initial concentration. In the first type, the suspension settles with two interfaces. Beneath the upper interface, referred to as a regular shock wave, the characteristic lines all represent the same initial concentration. In the lower part of the settling curve the characteristic lines have a fan shape and show an increase in concentration towards the bottom. The characteristics in the upper part interfere with the characteristics in the lower part and, where they intersect, a second interface is formed, referred to as a compound shock wave. The zone between the two interfaces is called the hindered settling phase, while after the lower interface there is a ''fluid mud phase'' which evolves into the consolidation phase at $\phi \approx 1$. In the hindered settling and the ''fluid mud phase'' hindered settling takes place, while in the consolidation phase consolidation occurs.

FOIA_07123_0005563_0013

In the second type of settling only one interface is formed. In the upper part of the settling suspension the characteristics are parallel to each other and the concentration is uniform. Lower in the settling suspension the characteristics diverge from each other and the concentration gradually increases. This is referred to as a rarefaction wave. The characteristics do not intersect and a lower interface is not formed.

The method of characteristics works well for analysis of the experimental results. However, to test the new hindered settling equation, we also need a numerical model. For this purpose Eq. (16) was implemented in a 1DV model to deal with high concentration suspensions. In order to use the 1DV model, values of the model parameters had to be derived from the experiments. Therefore, another goal of this study was to assess these values. The relevant parameters are the gelling concentration (c_{gel}), the return flow parameter (m) and the settling velocity of single flocs in still water $(w_{s;0})$. The gelling concentrations were derived from conductivity measurements. This concentration was different for the various settling experiments, but always within the range of 66 and 90 kg/m^3, with a mean of about 81 − 8 kg/m^3. In the model we used the mean c_{gel}, but a sensitivity analysis was done using both the minimum and the maximum gelling concentrations. The model conformed to the data properly when the average gelling concentration was used, although the larger gelling concentration also predicted the data properly for $f_i \geq 0.7$. The parameter m was derived from the characteristic lines in combination with experimental results, showing that there could be either one or two interfaces, which resulted in $m \geq 1$. A further analysis of the flux function resulted in $m = 2$, which was used in the model. The value of $w_{s;0}$ was derived by calibrating the model against two experiments. The model showed to represent the data well. Therefore, we conclude that the hindered settling and the fluid mud phases of kaolinite suspensions can be described with:

$$w_s = w_{s;0} \frac{(1 - f)^2 (1 - f_p)}{1 + 2.5 f}, \qquad (21)$$

where for our experiments $f = c/c_{gel}$, $c_{gel} \approx 81 - 8$ kg/m^3, $f_p = c/r_s$ and $w_{s;0}$ from Table 2.

In contrast to the model of Richardson and Zaki (1954), this model allows easily for an extension to the (hindered) settling of highly concentrated mud–sand suspensions (with a low sand concentration), which is subject of further work. Moreover, Eq. (21) can be integrated with a description for consolidation in an advection–diffusion equation after which it will cover the entire range of settling to consolidation (e.g. Winterwerp and Van Kesteren, 2004).

Acknowledgements

This work was funded by the DIOC-Water Project, Transient Processes in Hydraulic Engineering and Geohydrology, of Delft University of Technology. The authors would like to express their appreciation to ir. W.G.M. van Kesteren and Prof. Dr. ir. M.J.F. Stive for their support, advice and suggestions. Furthermore, the comments and suggestions by Dr. G.C. Sills and an anonymous reviewer are highly appreciated.

References

Bartholomeeusen, G., De Sterck, H., Sills, G., 2003. Non-convex flux functions and compound shock waves in sediment beds. In: Hyperbolic Problems: Theory, Numerics, Applications: Proceedings of the Ninth International Conference on Hyperbolic Problems, pp. 347–356.

Been, K., 1980. Stress–strain behaviour of a cohesive soil deposited under water. Ph.D. Thesis, Oxford University.

Bustos, M., Concha, F., Bürger, R., Tory, E., 1999. Sedimentation and thickening. Phenomenological foundation and mathematical theory. In: Mathematical Modelling: Theory and Applications, vol. 8. Kluwer Academic Publishers, Dordrecht.

Dankers, P., Winterwerp, J., Van Kesteren, W., 2007. A preliminary study on the hindered settling of kaolinite flocs. In: J.P.-Y. Maa, L.P. Sanford, D.H. Schoellhamer (Eds.), Estuarine and Coastal Fine Sediments Dynamics, INTERCOH 2003, Proceedings in Marine Science. Elsevier, pp. 227–241.

Kranenburg, C., 1992. Hindered settling and consolidation of mud—analytical results. Technical Report 11–92, Delft University of Technology.

Kynch, G., 1952. A theory of sedimentation. Transactions of the Faraday Society 48, 166–176.

Lester, D.R., Usher, S.P., Scales, P.J., 2005. Estimation of the hindered settling function R(f) from batch-settling tests. A.I.Ch.E. Journal 51 (4), 1158–1168.

Mandersloot, W., Scott, K., Geyer, C., 1986. Sedimentation in the hindered settling regime. In: Muralidhare, H. (Ed.), Advances in Solid–Liquid Separation. Battle Press, pp. 63–77.

Mehta, A., 1986. Characterisation of cohesive sediment properties and transport processes in estuaries. In: Mehta, A. (Ed.), Estuarine Cohesive Sediment Dynamics, Lecture Notes in Coastal and Estuarine Studies. Springer, Berlin, pp. 290–325.

FOIA_07123_0005563_0014

Merckelbach, L., 2000. Consolidation and strength evolution of soft mud layers. Ph.D. Thesis, Delft University of Technology.

Richardson, J., Zaki, W., 1954. The sedimentation of a suspension of uniform spheres under conditions of viscous flow. Chemical Engineering Science 3, 65–73.

Scott, K., 1984. Hindered settling of a suspension of spheres; critical evaluation of equations relating settling rate to mean particle diameter and suspension concentration. Technical Report 497, Chemical Engineering Research Group, Pretoria, South Africa.

Sills, G., 1997. Hindered settling and consolidation in cohesive sediments. In: Burt, N., Parker, R., Watts, J. (Eds.), Cohesive Sediments (Intercoh 1994). Wiley, Chichester, pp. 107–120.

Toorman, E., 1992. Modelling of fluid mud flow and consolidation. Ph.D. Thesis, Katholieke Universiteit Leuven, Faculteit Toegepaste Wetenschappen.

Uittenbogaard, R., Winterwerp, J., Van Kester, J., Leepel, H., 1996. 3D cohesive sediment transport—a preparatory study about implementation in delft3d. Technical Report Z1022, Delft Hydraulics.

Winterwerp, J., 2002. On the flocculation and settling velocity of estuarine mud. Continental Shelf Research 22, 1339–1360.

Winterwerp, J., Van Kesteren, W., 2004. Introduction to the physics of cohesive sediment in the marine environment. In: Developments in Sedimentology, vol. 56. Elsevier, Amsterdam.

FOIA_07123_0005563_0015